USING LROC NAC-DERIVED SINGLE-SCATTERING ALBEDO TO COMPARE THE COMPOSITIONS OF NON-MARE SILICIC VOLCANISM ON THE MOON.

E. M. Culley[1] and B. L. Jolliff[1], [1]Department of Earth, Environmental, and Planetary Sciences and the McDonnell Center for the Space Sciences. (eculley@wustl.edu)

Introduction: Regions of non-mare silicic volcanism, identifiable by strong UV absorption [1-3], morphologically distinct features [e.g., 4-7], and spectra indicating thorium-rich, low-FeO, silicic material [e.g. 8-10], are rare across the lunar surface. Hypotheses for their formation mechanisms are debated. Gaining further understanding of the compositions of these features, particularly the distribution and degree of silica enrichment at these sites will help constrain potential formation scenarios.

We compute the single-scattering albedo (SSA) of two non-mare silicic volcanism regions: Gruithuisen Gamma Dome (GD) (36.6°N, 40.7°W) and Compton-Belkovich Volcanic Complex (CBVC) (61°N, 99.5°E).

Methods and Data: We perform photometric analysis using Narrow Angle Camera (NAC) images from the Lunar Reconnaissance Orbiter Camera (LROC) [11] to determine the single-scattering albedo (SSA) of regolith across the CBVC and GD. Using Hapke photometric modeling [12] combined with NAC-derived digital terrain models (DTMs) [13], we account for local incidence and emission at every pixel to determine SSA at very high resolutions (2 mpp).

Fig. 1a and 1b show the calculated SSA for the CBVC and GD respectively, with outlines indicating topographic and morphologic units within each region. Within the CBVC, SSA values range depending on morphologic unit, whereas the GD summit plateau shows variation in SSA values. Further, the SSA values of the CBVC are mostly higher than those of the GD summit plateau. Inferring composition from SSA [2], we evaluate the composition of features within each region and differences between the two regions.

Results and Discussion: Fig. 1c shows the average SSA of distinct morphologic regions across and around the CBVC and GD. Both the CBVC and GD display elevated SSA compared to their respective surroundings. The CBVC caldera shows the highest SSA values, CBVC ridges show moderately high SSA, while the Alpha dome exhibits the lowest SSA within the CBVC. Interestingly, even the highest SSA values in GD are lower than those in the CBVC, although they also show a range of values. Thus, our data suggest that the CBVC is more silicic than Gruithuisen Gamma Dome.

Conclusions: Using LROC NAC geometric stereo image sets and corresponding DTMs, we determine the SSA of the CBVC and GD at high resolution. Values of SSA across the CBVC indicate silicic compositions ranging from rhyolitic in the central caldera to dacitic across the ridges and perhaps andesitic on the alpha dome. The GD summit plateau contains values lower than the CBVC Alpha dome, suggesting a more andesitic composition or mixing with a higher FeO source.

Acknowledgments: We thank NASA for support of the LRO extended mission and the LRO & LROC Operations Teams for their hard work. Additional thanks to the LROC Photometry Group and colleagues at ASU for NAC DTMs.

References: [1] Whitaker E. (1972) *Moon* **4**, 348-355. [2] Clegg-Watkins R. et al. (2017) *Icarus* **285**, 169-184. [3] Braden S. et al. (2010) *LPSC* **41**, #2677. [4] Hawke B.R. et al. (2003) *JGR-P* **108**, 5069. [5] Jolliff B. et al. (2011) *Nat Geosci* **4**, 566-571. [6] Glotch T. et al. (2011) *GRL* **38**, L21204. [7] Ivanov M. et al. (2016) *Icarus* **273**, 262-283. [8] Lawrence D. et al. (2000) *JGR* **105**, 307-320. [9] Hagerty J. et al. (2006) *JGR* **111**, E06002. [10] Glotch T. et al. (2010) *Science* **329**. 1510-1513. [11] Robinson M. et al. (2010) *Space Sci Rev* **150**, 81-124. [12] Hapke B. (2012b) *Theory of Reflectance and Emittance Spectroscopy* (2nd Ed). [13] Henriksen M. (2017) *Icarus* **283**, 122-137.

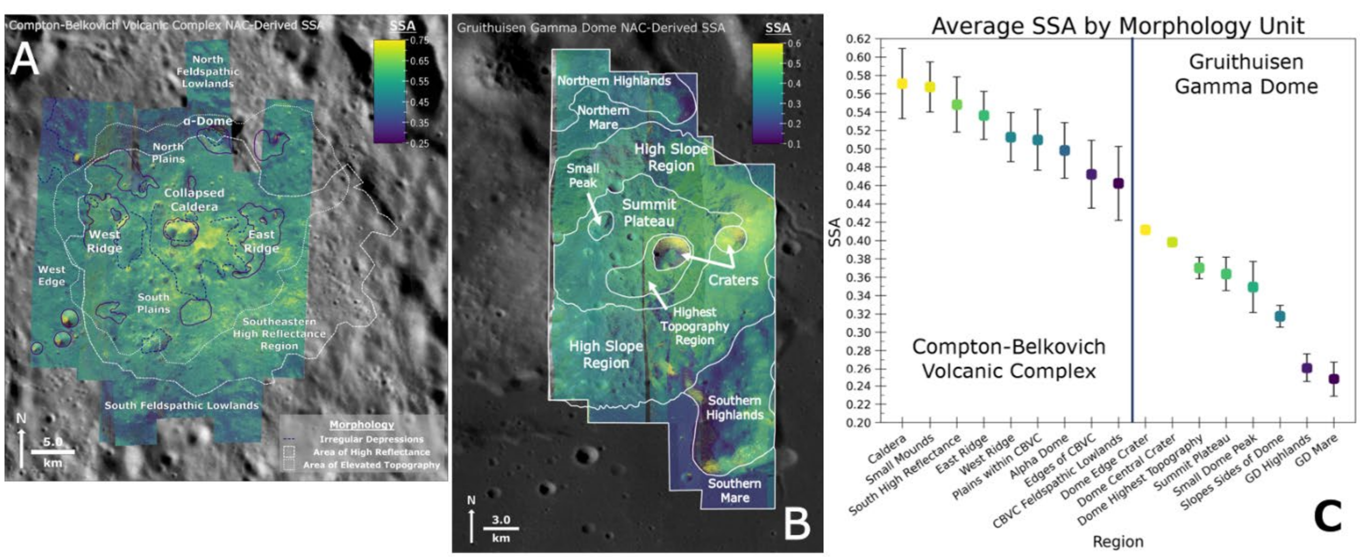

Figure 1. a) Map of SSA across CBVC with complex boundaries and important volcanic features outlined. b) Map of SSA across GD with morphologic units. c) Plot of average SSA across primary morphologies for both analysis regions.